NANO: Brief Reports and Reviews
Vol. 1, No. 1 (2006) 77–85

World Scientific
www.worldscientific.com

THE EFFECT OF SINGLE WALL CARBON NANOTUBES ON THE DIPOLE ORIENTATION AND PIEZOELECTRIC PROPERTIES OF POLYMERIC NANOCOMPOSITES

JIN HO KANG* and CHEOL PARK†
National Institute of Aerospace
MS 226, NASA Langley Research Center, Hampton, VA 23681, USA
**j.h.kang@larc.nasa.gov*
†*c.park@larc.nasa.gov*

STEVEN J. GAIK
Department of Chemical Engineering, Pennsylvania State University
University Park, PA 16802, USA
sjg212@psu.edu

SHARON E. LOWTHER‡ and JOYCELYN S. HARRISON§
Advanced Materials and Processing Branch
NASA Langley Research Center
MS 226, Hampton, VA 23681, USA
‡*s.e.lowther@larc.nasa.gov*
§*j.s.harrison@larc.nasa.gov*

Received 6 June 2006
Revised 15 June 2006

Recently, a series of single wall carbon nanotube (SWNT) polyimide nanocomposites were developed since the demand of electroactive polymeric materials as sensors and actuators for use in high temperature applications has been growing. Adding SWNTs into electroactive polyimides enhanced their electrostrictive strain as well as their mechanical integrities and chemical stability. Although an increase in piezoelectricity resulting from the incorporation of SWNTs could be expected, there has been no systematic study detailing the effect of SWNTs on piezoelectricity. In this article, the effects of various types and concentrations of SWNT on the dipole orientation and piezoelectricity were investigated using a thermally stimulated current (TSC) technique and a modified Rheovibron. It was found that the barely modified SWNTs led to a more substantial increase in the remanent polarization (P_r) than the highly modified SWNTs did. As the loading level of SWNTs increased, P_r increased. However, excessive loading of SWNTs showed a reduction in P_r since the actual poling field decreased due to a large leakage of current. The trend of the piezoelectric strain coefficient, d_{31}, was consistent with that of P_r. The increase in interfacial polarization caused by adding SWNT was believed to be primarily responsible for the increase of P_r and d_{31}.

Keywords: Piezoelectricity; single wall carbon nanotube (SWNT); thermally stimulated current (TSC); dipole orientation; interfacial polarization.

†Corresponding author.

1. Introduction

Electroactive polymeric materials have been studied extensively during the last two decades for use in a variety of applications including electromechanical sensors and actuators, ultrasonic transducers, loudspeakers, sonars, medical devices, prosthetics, artificial muscles, and devices for vibration and noise control.[1–3] As compared to electroactive ceramics and shape memory alloys, electroactive polymeric materials offer a unique combination of qualities because they are lightweight, conformable, and tough. Recently, we have developed a series of amorphous piezoelectric polyimides containing polar functional groups based on molecular design and computational chemistry, for potential use as sensors in high temperature applications.[4–6] One of these, an electroactive polymer containing a single nitrile group, (β-CN)APB/ODPA polyimide, retains more than 50% of its room temperature remanent polarization at 150°C for 500 h while maintaining its impressive mechanical characteristics.[7] The piezoelectric response of this polyimide is, however, an order of magnitude smaller than that of polyvinylidene fluoride (PVDF). This is due to the fact that the dipoles in the polymer do not align along the applied electric field efficiently because of limited chain mobility within the imidized closed ring structure. To increase the piezoelectric response of these polymers, synthesis of new polymers with various monomers[6] and control of the poling process[7] were reported.

In this article, we report the effect of types and concentrations of SWNT on the dipole orientation of the (β-CN)APB/ODPA polyimide by analyzing the thermally stimulated current (TSC) spectra. Also, a discussion of the piezoelectric properties measured using a modified Rheovibron will be addressed.

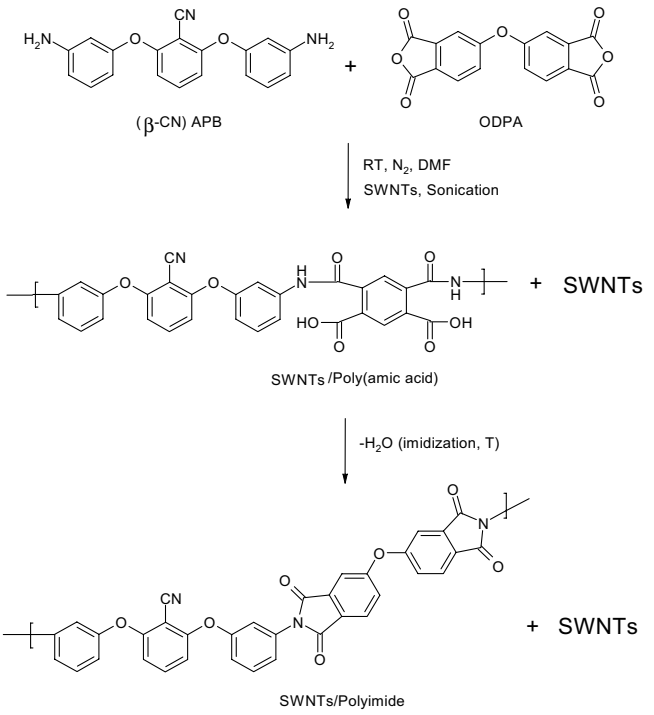

Fig. 1. Schematic diagram of synthesis of SWNT/polyimide nanocomposite.

2. Experimental

2.1. *Materials*

The SWNT/(β-CN)APB/ODPA polyimide (SWNT/polyimide) nanocomposite was prepared by *in situ* polymerization under sonication and mechanical shear (Fig. 1). The (β-CN)APB/ODPA polyimide was synthesized as a matrix from a diamine, 2,6-bis(3-aminophenoxy) benzonitrile ((β-CN)APB), and a dianhydride, 4,4'-oxydiphthalic anhydride (ODPA). The purified HiPCO (High-Pressure CO Conversion)-SWNTs were purchased from Carbon Nanotechnologies, Inc. and used as received. The surface modified SWNTs, P2- and P3-SWNTs were obtained from Carbon Solution, Inc. and used as received. The P2- and P3-SWNTs were treated with a strong acid moderately and highly, respectively. The detailed information of SWNTs used in this study is summarized in Table 1. The concentrations of SWNT in the polyimide varied from 0 wt% to 0.2 wt%. The complete synthetic procedure is described in detail elsewhere.[8] The uniform thickness (about 50 μm) of composite films was controlled by a solution cast technique on a glass plate with a doctor's blade. Sample dimensions for measurements are described in the characterization section.

2.2. *Poling procedure*

Film specimens were poled using a conventional poling procedure in an environmental oven. Each sample was polarized by a DC electric field of 30–60 MV/m. Optimal E_p depends on samples. For example, E_p of 60 MV/m was used for pristine polyimide, while E_p of 30 MV/m was used for a 0.02 wt% HiPCO nanocomposite at an elevated temperature ($T_p = T_g + 5$°C) for a selected poling time ($t_p = 30$ min). The details of the

Table 1. The characteristics of single wall carbon nanotubes (SWNTs) used.

SWNT	Preparing method	Chemical modification	Conductivity	Ref.
HiPCO	HiPCO process	Negligible	High	A
P2	Electronic arc method	Moderately	Medium	B
P3	Electronic arc method	Highly	Low	B

A. Carbon Nanotechnologies, Inc., http://www.cnanotech.com.
B. Carbon Solution, Inc., http://carbonsolution.com/.

conventional poling procedures have been described elsewhere.[9]

2.3. *Characterization*

Raman scattering spectra were obtained using an Almega^{TM} dispersive visible Raman spectrometer (Thermo Nicoltet). A 785-nm incident laser light excitation with a 25-μm-slit aperture was used and the laser beam was focused on the sample using an optical microscope. Low excitation laser power (10 mW) was used to minimize heating of the samples, since heating often caused a downshifting in the observed peaks.

The dielectric constant and the AC conductivity of the pristine polyimide and the SWNT nanocomposites were measured using an HP 4291A impedance analyzer and a Novocontrol system as a function of frequency. Disk-shaped films (25.4 mm-diameter) were employed for the AC measurements. The DC conductivity was measured with a Keithley 6517 electrometer and a Keithley 8009 high resistance test fixture. Square films (10 cm × 10 cm) were used for the DC conductivity measurement.

The remanent polarization (P_r) was measured as a function of temperature, after poling. The sample was a 10 mm × 10 mm film shape. As the sample was heated through its glass transition temperature (T_g) at a heating rate of 10.0°C/min, the depolarization current was measured using a Setaram TSC-II. The remanent polarization (P_r), equal to the charge per unit area, was derived by integrating the current with respect to time and plotting it as a function of temperature. This is given by,

$$P_r = \frac{q}{A} = \frac{1}{A}\int I(t)dt\,, \tag{1}$$

where q is the charge, A is the electrode area, I is the current, and t is the time.

Piezoelectric strain coefficient, d_{31}, was measured using a modified Rheovibron. Rectangular film specimens were used with the dimension of a 30 mm × 5 mm. The sample was subjected to in-plane stress (1-direction or length direction), F/wt, resulting in charge, q, through the film thickness (3-direction or out-of-plane direction). The piezoelectric strain coefficient was calculated according to the following equation:

$$d_{31} = \frac{(q/wl)}{(F/wt)}\,, \tag{2}$$

where q is charge, w is the width of the sample, l is the length, F is applied force and t is the thickness. The coefficient d_{31} was measured at 1 Hz and as a function of temperature from 25°C to 150°C.

3. Results and Discussion

To study the effect of SWNT type and concentration on dipole orientation and piezoelectric properties of an electroactive polyimide, three types of SWNTs were dispersed into the polyimide and processed into free-standing films. As shown in Table 1, the HiPCO-SWNTs were subjected to a mild acid treatment for purification and annealed to heal the damaged nanotube surface. However, the P2- and P3- SWNTs were treated with a strong acid moderately and highly, respectively, resulting in modification of the nanotube surface chemistry and electrical conductivity. The electronic nature of the different types of SWNTs was examined using Raman spectroscopy. Figure 2 presents the Raman spectra of the SWNT nanocomposites ((a) HiPCO, (b) P2, and (c) P3 nanocomposites). Noticeable differences among the spectra are observed at the peaks of their tangential G (at $\sim$1590 cm^{-1}) and radial breathing modes (RBM) (at $\sim$200 cm^{-1}). The spectrum of 0.1 wt% HiPCO nanocomposite displays sharp peaks of the SWNT tangential G mode and the radial breathing modes.[10–12] Whereas, these peaks are weaker for the P2 and P3 nanocomposites. The smaller peak of the tangential mode indicates that some of the sp^2 electron orbital structure partially converted to sp^3 electron orbital structure due to the acid treatment. SWNTs with less sp^2 structure are known to have

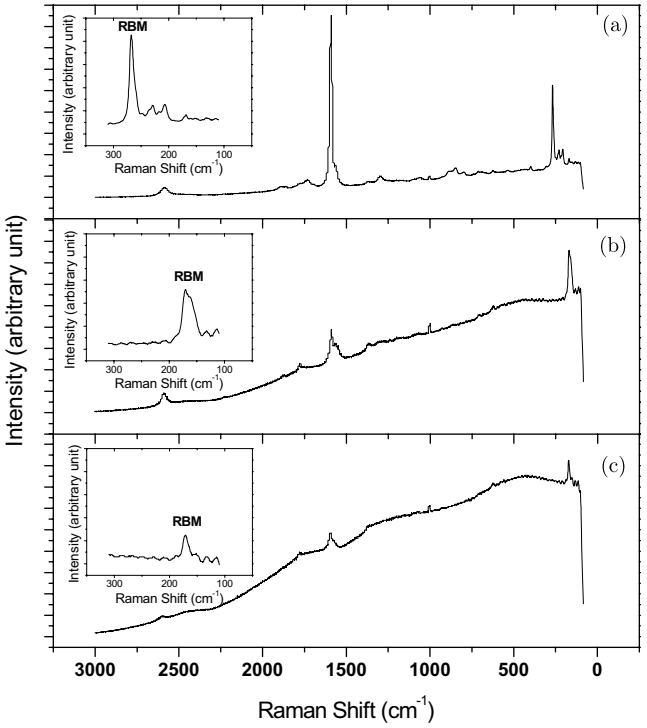

Fig. 2. Raman spectra of SWNT/polyimide nanocomposites: (a) 0.1 wt% HiPCO-SWNT, (b) 0.1 wt% P2-SWNT, and (c) 0.1 wt% P3-SWNT. A 785-nm (1.58 eV) incident laser light excitation with a 25-μm-slit aperture was used.

lower electrical conductivity due to a drastic reduction in their delocalized π-electron density and higher fluorescence. The greater slopes toward the low wavenumber in Figs. 2(b) and 2(c) are associated with fluorescence.[10,13] Conversely, SWNTs with fewer sp^3 electron orbitals are known to have higher electrical conductivity and less fluorescence since they behave like nonradiative channels during the electron excitation process.[14,15] Through the nonradiative channels, the electrons excited by photons transfer to adjacent conduction bands rather than to the unexcited states to emit fluorescence. In addition, from the RBM peaks in Fig. 2, the nanotube diameter (D) can be estimated by the following equation of RBM frequency (ω):

$$\omega\ (\mathrm{RBM}) = \frac{\alpha}{D}\,, \tag{3}$$

where the proportionality constant, $\alpha = 248\,\mathrm{cm}^{-1}\,\mathrm{nm}$ was used.[11,12] The diameter of HiPCO-SWNT (~ 0.92 nm) was smaller than those of P2- and P3-SWNTs (~ 1.44 nm and ~ 1.48 nm, respectively) since the SWNTs were prepared by different methods as noted in Table 1. It was also important to note that SWNTs with smaller radii were more readily destroyed during the acid treatment than those with larger radii.

Significant differences in the electrical conductivity and the dielectric constant of the SWNT nanocomposites were observed as shown in Fig. 3.

The AC electrical conductivities of the pristine polyimide and the 0.2 wt% P3 nanocomposite were linear as a function of frequency on a logarithmic scale. This linear correspondence is typical for insulators and indicates that the percolation threshold for the P3-SWNT was not achieved at this concentration. Conversely, the AC conductivities of 0.2 wt% P2 and 0.2 wt% HiPCO nanocomposites were much higher. The constant conductivity for a

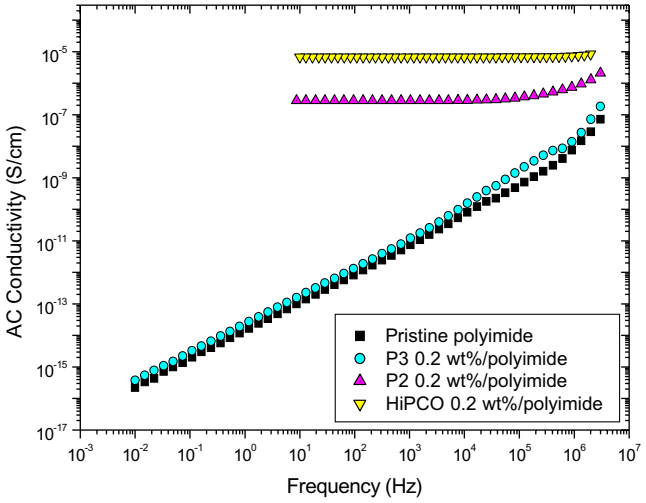

(a)

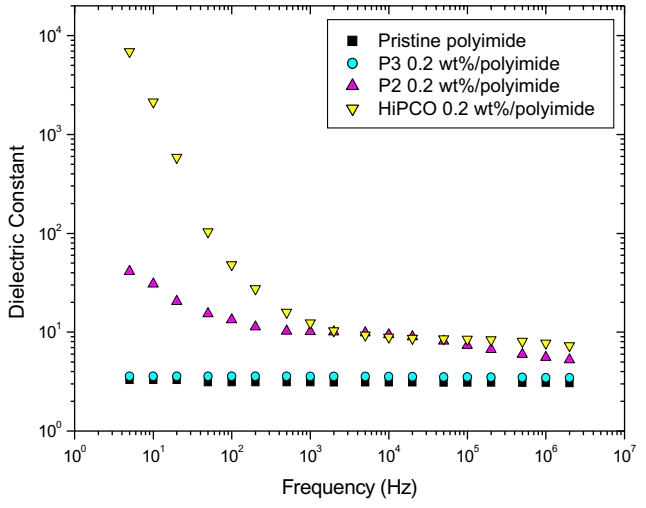

(b)

Fig. 3. (a) AC electrical conductivity and (b) dielectric constant of 0.2 wt% SWNT/polyimide nanocomposite.

broad range of frequencies for these nanocomposites shown in Fig. 3(a) indicates that the percolation threshold was exceeded thus rendering the materials conductive. The nanocomposite with SWNTs with minimal acid treatment exhibited higher conductivities, which is consistent with the Raman spectra in Fig. 2.

The effect of SWNTs on the dielectric constant of the nanocomposites showed a similar trend to that of the SWNTs on the conductivity as shown in Fig. 3(b). The dielectric constant of the nanocomposites decreased with increasing degree of surface treatment. In particular, the 0.2 wt% HiPCO nanocomposite showed a large increase in the dielectric constant at a relatively low frequency ($\varepsilon \sim 6900$ at 5 Hz). This increase is indicative of the presence of interfacial polarization.[16–19] Interfacial polarization occurs when charges accumulate at the interfaces between inclusions and the host matrix. This leads to field distortion and gives rise to dipole moments. This effect is prevalent at low frequencies since the dipole relaxation time of this type of polarization is large. In our system, there were abundant nanotube polymer interfaces, which results in significant interfacial polarization. This interfacial polarization was believed to be responsible for the increase in the dielectric constant. The dielectric constant of the HiPCO nanocomposite was higher than those of highly acid-treated SWNT nanocomposites accordingly. Figure 4 shows the conductivity and the dielectric constant of the nanocomposites with 0.02 wt% SWNTs. The addition of a small amount of SWNT moderately increased the conductivity and dielectric constant of the nanocomposite, with the HiPCO-SWNT showing the highest as expected. Since the concentration of SWNTs was very low (0.02 wt%), percolation was not achieved.

Figure 5 shows the electrical conductivity and the dielectric constant of the P3 nanocomposites as a function of nanotube concentration. Both conductivity and dielectric constant of the nanocomposites increased with increasing SWNT concentration. All the samples even up to 0.2% of P3-SWNT exhibited nonconducting nature below percolation. Note that a typical volume fraction (ϕ_c) of the percolation threshold of HiPCO (highly conductive SWNTs) nanocomposite was less than 0.06%.[20,21] Because P3-SWNT was highly modified with the acid treatment and consequently less conductive, the nanocomposite incorporated with even 0.2 wt% P3-SWNT also

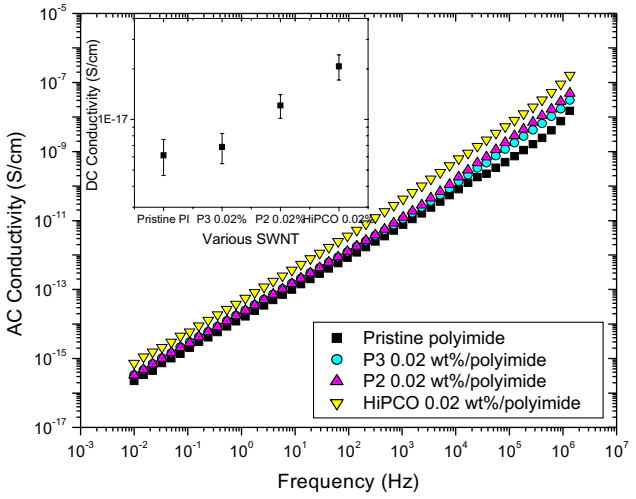

(a)

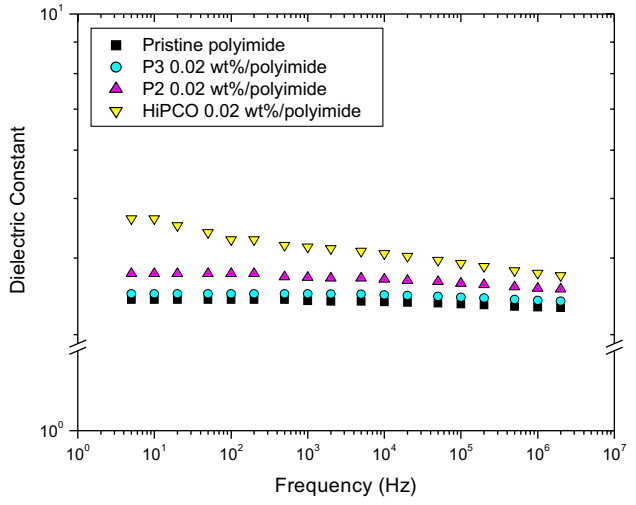

(b)

Fig. 4. (a) AC and DC electrical conductivity and (b) dielectric constant of 0.02 wt% SWNT/polyimide nanocomposites.

fell below the percolation threshold. An inset in Fig. 5(a) shows the DC electrical conductivity of P3 nanocomposites as a function of nanotube concentration. Even though these nanocomposites remained below percolation up to 0.2 wt% concentration, the conductivities increased with increasing P3-SWNT concentration over five times of the magnitude of the conductivity of the pristine polymer. Figure 5(b) shows the effect of the concentration of SWNTs on AC dielectric constant as a function of frequency. The dielectric constant increased gradually with increasing P3-SWNT concentration reached over 4 at a 0.2 wt% P3-SWNT concentration.

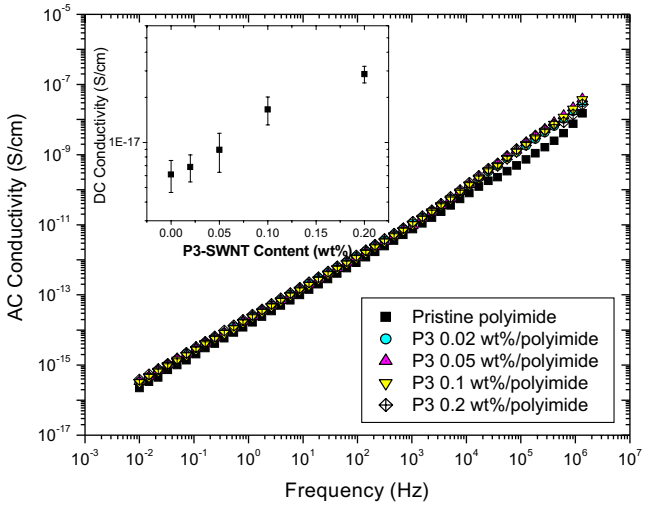

(a)

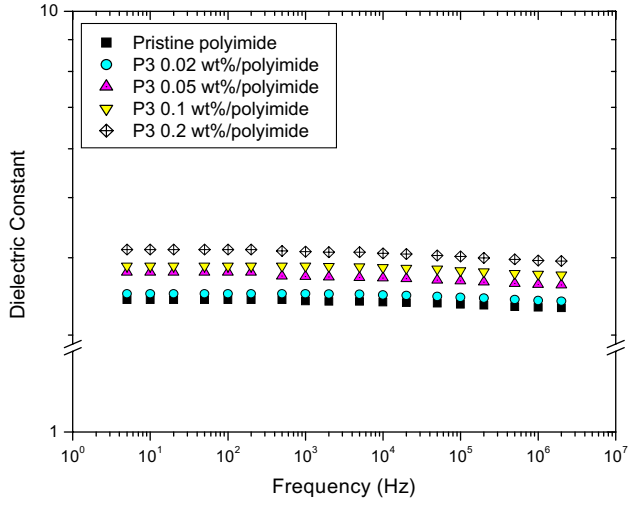

(b)

Fig. 5. (a) AC and DC electrical conductivity and (b) dielectric constant of P3-SWNT/polyimide nanocomposites.

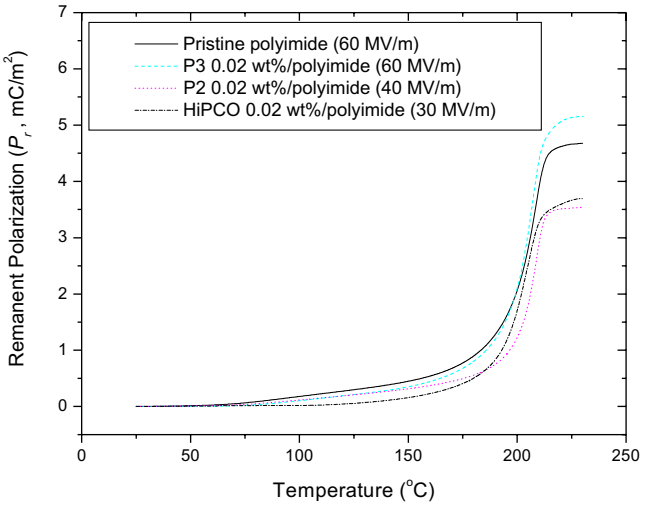

(a)

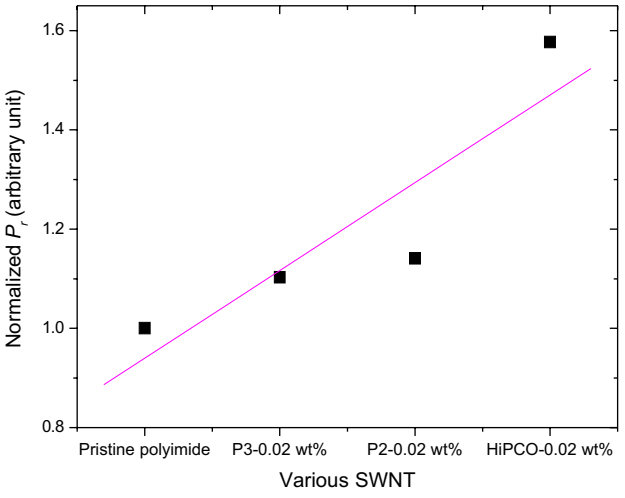

(b)

Fig. 6. (a) Remanent polarization (P_r) calculated from thermally stimulated current (TSC) and (b) normalized remanent polarization (P_r) of 0.02 wt% SWNT/polyimide nanocomposites.

To study the effect of SWNT type on the polarization and piezoelectric properties, the nanocomposites were poled. Previous work with the pristine polyimide has shown that optimal poling conditions are achieved at T_p (poling temperature) $= T_g + 5°\mathrm{C}$ and t_p (poling time) of 30 min. For the SWNT nanocomposites, it was necessary to optimize poling field strength, E_p. An electric field of 60 MV/m was used for the pristine polyimide. It was necessary to lower the electric field strength for the SWNT nanocomposites to avoid dielectric breakdown. Using TSC, the remanent polarization (P_r) was calculated according to Eq. (1), which is shown in Fig. 6(a).[22,23] The P_r of pristine polyimide was 4.7 mC/m^2. To examine the relative effect of the types of SWNTs on P_r, the measured P_r values were normalized by the poling field. As shown in Fig. 6(b), the normalized P_r of all the SWNT nanocomposites was higher than that of the pristine polyimide. Moreover, the more conductive SWNTs (less acid treatment) resulted in higher remanent polarization. The normalized P_r of 0.02 wt% HiPCO nanocomposite was 58% higher than that of the pristine polyimide.

The piezoelectric strain coefficients, d_{31}, are shown in Fig. 7(a) as a function of temperature

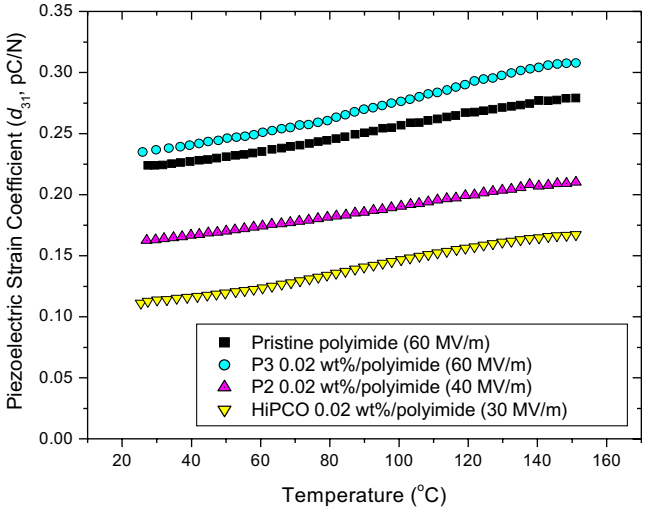

(a)

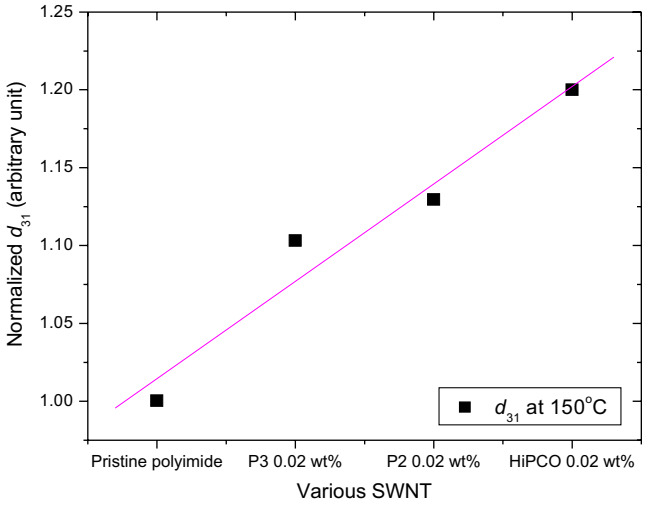

(b)

Fig. 7. (a) Piezoelectric strain coefficient (d_{31}) as a function of temperature and (b) normalized piezoelectric strain coefficient (d_{31}) of pristine polyimide and 0.02 wt% SWNT/polyimide nanocomposites.

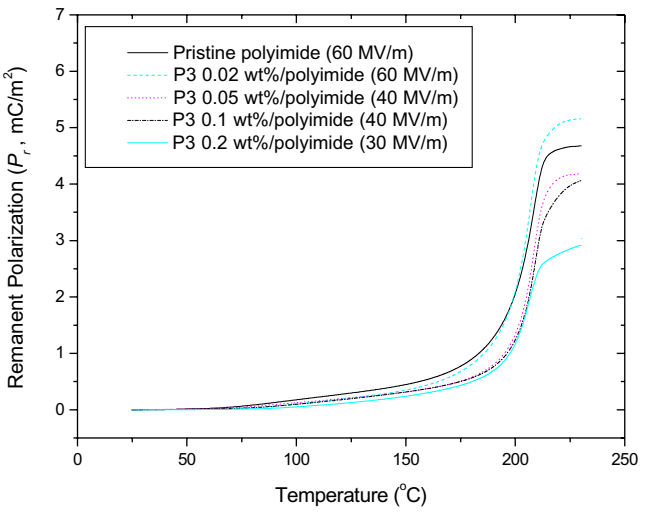

(a)

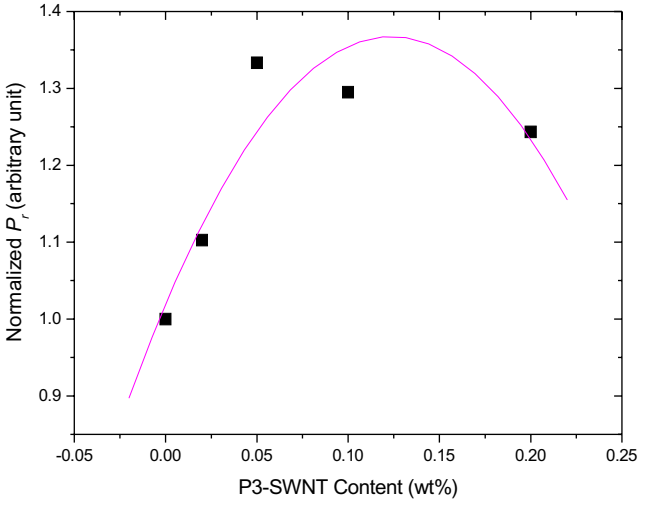

(b)

Fig. 8. (a) Remanent polarization (P_r) calculated from thermally stimulated current (TSC) and (b) normalized remanent polarization (P_r) of P3-SWNT/polyimide nanocomposites.

for the SWNT nanocomposites. The d_{31} increased slightly with increasing temperature due to a decrease in the modulus. Figure 7(b) shows the d_{31} (at 150°C) normalized by the poling field. The trend of normalized d_{31} was consistent with that of the normalized P_r. The more conductive SWNTs led to the greater d_{31} due to the higher dipole orientation resulting from the interfacial polarization of the nanocomposites.

The P3-SWNT, the least conductive SWNT, was employed for the study of SWNT concentrations. Figure 8 shows the remanent polarization (P_r) calculated from TSC of P3 nanocomposites. The normalized P_r increased with increasing SWNT content to show a maximum P_r value at 0.1 wt% of SWNT, and decreased with further loading of SWNTs (Fig. 8(b)). The decrease in the P_r above 0.1 wt% P3 nanocomposite originated from a lower actual poling field due to a high leakage of current. The normalized P_r of the 0.1 wt% P3 nanocomposite was 30% higher than that of the pristine polyimide. Similarly, the normalized d_{31} shown in Fig. 9 increased more than 20% than that of the pristine polyimide. The increase in P_r and

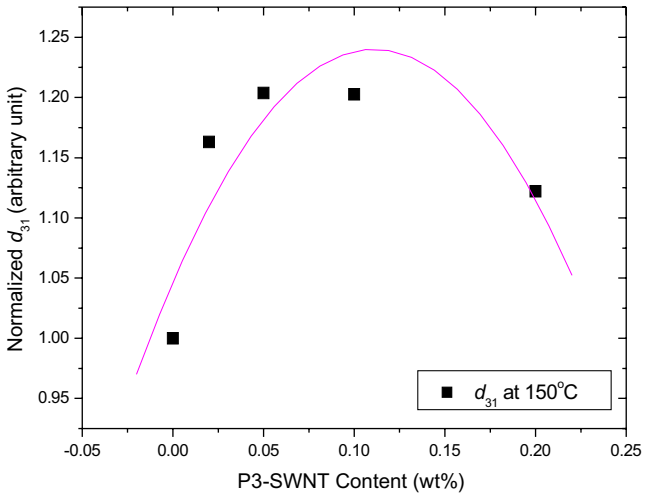

Fig. 9. Normalized piezoelectric strain coefficient (d_{31}) of P3-SWNT/polyimide nanocomposites as a function of SWNT concentration.

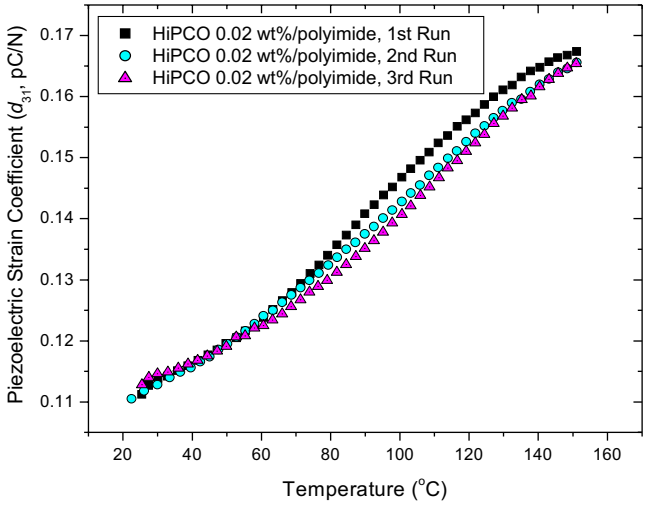

Fig. 10. Piezoelectric strain coefficient (d_{31}) of 0.02 wt% HiPCO-SWNT/polyimide nanocomposites as a function of temperature for three cycles.

d_{31} appear to be due to the higher dipolar orientation resulting from the interfacial polarization of the SWNT nanocomposite.

Figure 10 shows a cyclic measurement of d_{31} of the HiPCO nanocomposite as a function of temperature up to 150°C. The d_{31} values did not change after even three cycles, which indicated that the dipolar orientation was very stable at high temperatures up to 150°C. Therefore, the SWNT nanocomposites can be a good candidate for high temperature applications.

4. Conclusion

The effect of degree of the acid treatment on the conductivity and dielectric properties of nanocomposites were studied. Both conductivity and dielectric constant decreased with decreasing sp^2 nature of the SWNTs caused by acid treatment. The effect of the SWNT type and concentration on the dipole orientation and piezoelectric properties of the electroactive polymide was studied by measuring the thermally stimulated current (TSC) and the piezoelectric strain coefficient. The normalized P_r of the SWNT/polyimide nanocomposites decreased with increasing degree of the acid treatment. The normalized P_r increased with increasing SWNT concentration to show a maximum value at 0.1 wt% of SWNT loading and decreased with further loading of P3-SWNTs. The trend of the piezoelectric strain coefficient, d_{31}, was consistent with that of P_r. The higher dipole orientation resulting from the interfacial polarization of the SWNT/polyimide nanocomposite appeared to be the origin of the increase of P_r and d_{31}. From the cyclic piezoelectric measurement at a high temperature, it was found that the SWNT nanocomposites possess very thermally stable piezoelectric properties, applicable for high temperature devices.

Acknowledgments

The authors thank Gregory K. Draughon and Nancy M. Holloway for their help in preparation of electrode-deposited film. Park appreciates NASA University Research, Engineering and Technology Institute on Bio Inspired Materials (BIMat) under award no. NCC-1-02037 for support in part. Kang appreciates the Post-doctoral Fellowship Program of Korea Science and Engineering Foundation (KOSEF) under grant no. M01-2004-000-10344-0 for support in part.

References

1. K. Uchino, *Piezoelectric Actuators and Ultrasonic Motors* (Kluwer Academic, Boston, 1997).
2. Z. Ounaies, J. A. Young and J. S. Harrison, *Field Responsive Polymers*, eds. I. M. Khan and J. S. Harrison (ACS, Washington DC, 1999), pp. 88–103, Chapter 6.
3. Y. Bar-Cohen, *Electroactive Polymer (EAP) Actuators as Artificial Muscles-Reality, Potential, and Challenges* (SPIE, Bellingham, WA, 2001).

4. J. O. Simpson, S. S. Welch and T. L. St. Clair, *Proc. Mater. Res. Soc. Symp.*: *Mater. Smart Systems II* **413**, 351 (1995).
5. J. O. Simpson, S. S. Welch and T. L. St. Clair, *Proc. Mater. Res. Soc. Symp.*: *Mater. Smart Systems II* **459**, 59 (1997).
6. Z. Ounaies, C. Park, J. S. Harrison, J. G. Smith, Jr. and J. Hinkley, *Proc. SPIE Smart Struct. Mater.* **3669**, 171 (1999).
7. C. Park, Z. Ounaies, J. Su, J. G. Smith, Jr. and J. S. Harrison, *Proc. Mater. Res. Soc. Symp.*: *Mater. Smart Systems II* **600**, 153 (1999).
8. C. Park, Z. Ounaies, K. Watson, R. E. Crooks, J. Smith, Jr., S. Lowther, J. W. Connell, E. J. Siochi, J. S. Harrison and T. L. St. Clair, *Chem. Phys. Lett.* **364**, 303 (2002).
9. C. Park, Z. Ounaies, K. E. Wise and J. S. Harrison, *Polymer* **45**, 5417 (2004).
10. V. N. Popov, *Mater. Sci. Eng. R* **43**, 61 (2004).
11. A. Jorio, R. Saito, J. H. Hafner, C. M. Lieber, M. Hunter, T. McClure, G. Dresselhaus and M. S. Dresselhaus, *Phys. Rev. Lett.* **86**, 1118 (2001).
12. M. S. Dresselhaus, G. Dresselhaus, A. Jorio, A. G. S. Filho and R. Saito, *Carbon* **40**, 2043 (2002).
13. H. Dai, *Surf. Sci.* **500**, 218 (2002).
14. T. Belin and F. Epron, *Mater. Sci. Eng. B* **119**, 105 (2005).
15. M. J. O'Connell, S. M. Bachilo, C. B. Huffman, V. C. Moore, M. S. Strano, E. H. Haroz, K. L. Rialon, P. J. Boul, W. H. Noon, C. Kittrell, J. Ma, R. H. Hauge, R. B. Weisman and R. E. Smalley, *Science* **297**, 593 (2002).
16. C. C. Ku and R. Liepins, *Electrical Properties of Polymers* (Hanser Publishers, New York, 1987), pp. 20–58.
17. R. W. Sillars, *J. Inst. Elect. Engineers* **80**, 378 (1937).
18. H. Kawai, *Oyo Buturi* **41**, 461 (1972).
19. I. Bunget and M. Popesco, *Physics of Solids Dielectrics* (Elsevier Science, New York, 1984).
20. D. S. McLachlan, C. Chiteme, C. Park, K. E. Wise, S. E. Lowther, P. T. Lillehei, E. J. Siochi and J. S. Harrison, *J. Polym. Sci. Part B*: *Polym. Phys.* **43**, 3273 (2005).
21. S. Barrau, P. Demont, A. Peigney, C. Laurent and C. Lacabanne, *Macromolecules* **36**, 5187 (2003).
22. J. P. Runt and J. J. Fitzgerald, *Dielectric Spectroscopy of Polymeric Materials*: *Fundamentals and Applications* (American Chemical Society, Washington DC, 1997).
23. G. Teyssèdre, P. Demont and C. Lacabanne, *J. Appl. Phys.* **79**, 9258 (1996).